Control of the morphology of polyamide/styrene–acrylonitrile copolymer blends via reactive compatibilizers

B. Majumdar, H. Keskkula and D. R. Paul*
Department of Chemical Engineering and Center for Polymer Research, University of Texas at Austin, Austin, TX 78712, USA

and N. G. Harvey
Corporate Exploratory Research, Rohm and Haas Co., PO Box 219, Bristol, PA 19007, USA
(Received 12 November 1993; revised 10 March 1994)

The effects of several different compatibilizing agents with reactive functional groups (acid and/or anhydride) on the morphology of blends of styrene–acrylonitrile copolymers (SAN) in polyamide (PA) matrices were investigated using transmission electron microscopy. The primary focus was on the use of a series of imidized acrylic polymers and how their functionality for reaction with nylon-6 and their miscibility with SAN copolymers affected the morphology of nylon-6/SAN blends. Glass transition behaviour of binary blends of the imidized acrylic polymers with SAN systems indicated that miscible blends over a restricted range of AN content in the SAN could be obtained by limiting the imide and free-acid contents of the imidized acrylic polymers. In the case of the ternary polyamide blends, the most efficient reduction in the dispersed-phase particle size was obtained via imidized acrylic polymers that are miscible with the SAN phase and can react with the polyimide to a significant degree. For nylon-6/SAN blends compatibilized with polymers containing a high level of anhydride functionality, complex morphologies consisting of at least two distinct populations of dispersed phase were observed. The factors responsible for generation of such complex morphologies were examined using different staining techniques, and it was proposed that a rheological effect is the dominant issue. The chemical functionality characteristics of the polyamide matrix were also shown to have an effect on the morphology of nylon/SAN blends compatibilized with imidized acrylic polymers.

(Keywords: polyamide blends; imidized acrylic polymers; morphology)

INTRODUCTION

The control of morphology in multiphase blends through reactive compatibilization has been addressed in several recent publications[1–5]. In addition to processing and rheological issues[6–10], some of the key factors that influence the formation of block or graft copolymers via interfacial reaction during melt blending relate to the type of functional groups incorporated, the manner in which they are incorporated (grafted, comonomer, or terminal groups), molecular architecture, spacing and concentration of these functional groups, molecular weight of the chain to which these functional groups are attached, and the miscibility of the functional polymer with the major components of the blend. The work described here is motivated by the current interest in compatibilized blends of polyamide (PA) and acrylonitrile–butadiene–styrene (ABS) materials[11–18] and focuses on some of the issues mentioned above. These are complex systems since ABS is itself a two-phase material, which can vary considerably in rubber content and particle morphology[14]. Isolating the role of the nature of the compatibilizer in creating usefully tough alloys amid all these variables can be quite difficult. This paper begins a series of reports aimed at systematically examining some of the most important issues.

The first goal is to define the effectiveness of a series of compatibilizers, primarily imidized acrylic polymers, for control of the morphology of such blends via their reaction with the polyamide to form block or graft copolymers *in situ*. We simplify the problem here by using the styrene–acrylonitrile (SAN) copolymer matrix without any rubber phase.

Future papers will attempt to correlate the ability of a series of imidized acrylic polymers to manipulate the morphology of the nylon/SAN blends described here with the morphology and properties generated in more complex nylon/ABS systems. As described in more detail in the following section, the imidized acrylic materials are quite versatile in that they may have useful functionality for reaction with the amine end-groups of the polyamide and they may also be miscible with the SAN phase[19] of ABS materials. The objective here is to examine the relationship between the molecular design of these and other functionalized copolymers *versus* their effectiveness for controlling the morphology of polyamide blends with SAN copolymers.

* To whom correspondence should be addressed

0032-3861/94/20/4263–17

BACKGROUND

Although the techniques for synthesis of imidized acrylic polymers (also referred to in the literature as polyglutarimides or polymethacrylimides) have been known for some time[20–24], it is only recently that continuous reactive extrusion/devolatilization processes have been developed to generate such polymers based on the reaction between poly(methyl methacrylate) (PMMA) and methylamines at sufficiently high pressures and temperatures[25–28]. The complex reaction mechanism of this process involves alkyl–oxygen cleavage in the PMMA leading to the formation of at least four different types of chemical functionalities in a typical operation as shown in *Figure 1*. In addition to methyl glutarimide units, small amounts of methacrylic acid and glutaric anhydride units are generated, while some methyl methacrylate units remain unchanged. Owing to undesirable effects of the acid and anhydride groups for certain applications, re-esterification techniques have been developed to control the amount of acid and anhydride groups in these polymers[27,29].

Imidized acrylic polymers have high modulus, tensile strength and heat distortion resistance, which combined with their optical clarity make them attractive candidates for a number of uses[30–32]. More recently, the presence of controlled levels of acid and/or anhydride groups in these polymers has been utilized to generate blends with nylon via grafting reactions with the amine groups[33,34]. Depending on their functionality level, some of these polymers are miscible with SAN[19], which makes them potentially useful compatibilizers for nylon/SAN and nylon/ABS blends. Only brief reports on the applicability of these polymers in such systems have appeared to date[17].

In the work reported here, ternary blends of polyamide, SAN and a reactive imidized acrylic were melt compounded under conditions where reaction is possible. Depending on the molecular design of the imidized acrylic compatibilizer, one can anticipate at least three locations of the graft copolymer formed in these blends as shown schematically in *Figure 2*. If the imidized acrylic portion is fully miscible with the SAN phase, one may expect it to reside primarily within the SAN phase with its functional groups (A) forming chemical linkages to nylon chains at the interface as shown in *Figure 2a*. This situation is expected to lead to the most efficient reduction in the SAN domain particle size through a reduction in interfacial tension and increased steric stabilization (minimize coalescence). *Figure 2b* illustrates the situation where the functionalized compatibilizer is driven to the SAN interface because it has some thermodynamic affinity for this phase but not enough to be miscible with

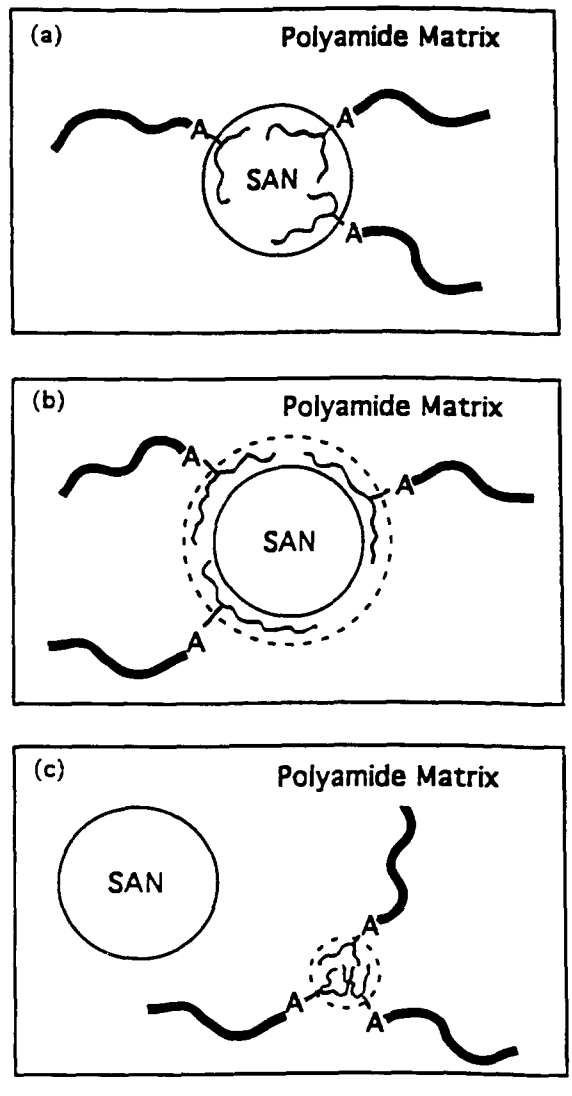

Figure 2 Schematic representation of three possible modes of location of graft copolymers formed by reaction of the imidized acrylic or compatibilizer chains (thin lines) with nylon-6 (thick lines) in SAN/polyamide blends

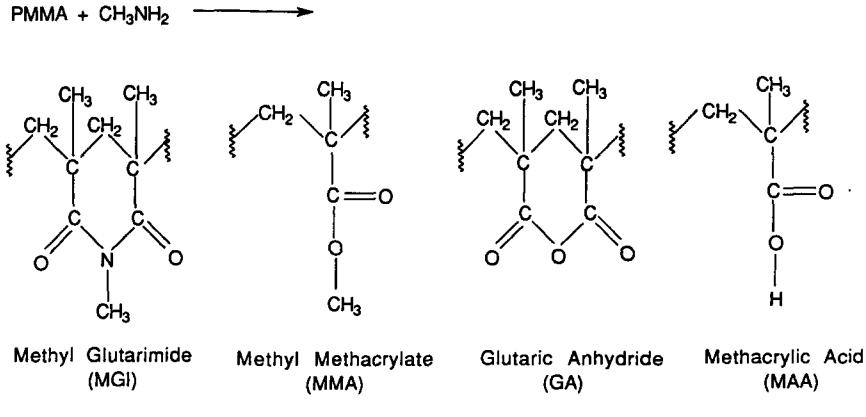

Figure 1 Main repeat units of imidized acrylic polymers formed by reactive extrusion of PMMA with methylamine

SAN. In this case, one can still expect some reduction in the SAN domain size for the same reasons mentioned above; however, this mode is not expected to be as ideal as that in *Figure 2a*. The third situation, *Figure 2c*, arises when the compatibilizer is even less attracted to the SAN phase, and, hence, resides in the polyamide phase away from the interface. This will not result in any strengthening of the polyamide/SAN interface or exert control over morphology in the ways expected for the previous two modes; however, the formation of these highly grafted micellar aggregates will increase the viscosity of the polyamide matrix, which may in turn lead to a change in the morphology of the blend[8,9]. In specific cases, combinations of the scenarios shown in *Figure 2* may best describe the actual situation in some ternary polyamide blends.

EXPERIMENTAL

The various polyamides, SAN copolymers and functionalized compatibilizers used in this study are shown in *Tables 1–3*. Of the six different polyamides used, three are homopolymers of nylon-6 while a fourth one is a homopolymer of nylon-6,6. The polyamide designated as XPN 1250 is a nylon-6 enriched in amine chain ends. Two copolymers of nylon-6 and nylon-6,6 have also been used. The nylon-6 used most extensively here is the one designated as Capron 8207F and will be referred to

Table 1 Polyamides used in this study

Polymer	Commercial designation	$\bar{M}_n$	End-group content (μeq g^{-1})		Relative melt viscosity[a]	Source
			NH_2	COOH		
Nylon-6	Capron 8207F	22000	47.9	43.0	1.0	Allied Signal Inc.
Nylon-6	XPN 1250	18000	73.0	17.2	0.8	Allied Signal Inc.
Nylon-6	B5	37000	28.1	23.8	3.3	BASF
Nylon-6,6	Zytel 101	17000	46.0	n.t.[b]	1.1[c]	E.I. du Pont Co.
Nylon-6/nylon-6,6 (85/15) copolymer	XPN 1539F	22000	52.7	50.1	1.1	Allied Signal Inc.
Nylon-6/nylon-6,6 (16/84) copolymer	Vydyne 86X	18000	46.6	64.7	1.0	Monsanto Chemical Co.

[a] Brabender torque at 240°C and 60 rev min^{-1} after 10 min divided by that of nylon-6
[b] Not tested
[c] Same as footnote *a*, except at 280°C

Table 2 Styrenic polymers used in this study

Polymer	Designation	*MW* information	Relative melt viscosity[a]	Source
Polystyrene	PS	$\bar{M}_n = 103000$ $\bar{M}_w = 341000$	0.8	Fina Oil and Chemical
Poly(styrene-*co*-acrylonitrile)				
5.7% AN	SAN 6	$\bar{M}_n = 88000$ $\bar{M}_w = 212000$	1.0	Asahi Chemical Co.
15.9% AN	SAN 16	$\bar{M}_n = 82000$ $\bar{M}_w = 173000$	0.9	Dow Chemical Co.
20% AN	SAN 20	$\bar{M}_n = 88000$ $\bar{M}_w = 178000$	1.2	Dow Chemical Co.
23% AN	SAN 23	$\bar{M}_n = 48200$ $\bar{M}_w = 92000$	0.3	Daicel Chemical Ind. Ltd.
25% AN	SAN 25	$\bar{M}_n = 77000$ $\bar{M}_w = 152000$	1.0	Dow Chemical Co.
26.7% AN	SAN 27	$\bar{M}_n = 46500$ $\bar{M}_w = 95000$	0.5	Daicel Chemical Ind. Ltd.
29.4% AN	SAN 29	$\bar{M}_n = 85400$ $\bar{M}_w = 163300$	1.2	Daicel Chemical Ind. Ltd.
34% AN	SAN 34	$\bar{M}_n = 73000$ $\bar{M}_w = 145000$	1.1	Asahi Chemical Co.
40% AN	SAN 40	$\bar{M}_n = 61000$ $\bar{M}_w = 122000$	1.3	Asahi Chemical Co.
Styrene/maleic anhydride[b,c] 25% MA	SMA 25	Viscosity = 4.73[d]	1.6	Monsanto Chemical Co.
Methyl methacrylate/styrene/maleic anhydride terpolymer (73/18/9)[c]	Delpet 980N	$\bar{M}_n = 61800$	1.7	Asahi Chemical Co.

[a] Brabender torque divided by that of nylon-6 (all at 240°C and 60 rev min^{-1} after 10 min)
[b] Contains a small amount of a third monomer
[c] Miscible with SAN 25
[d] Viscosity at 25°C (mPa s) of 10% solution in methyl ethyl ketone

Table 3 Imidized acrylic polymers used in this study

Designation[a]	T_g (°C)	Relative melt viscosity[b]	Methyl glutarimide (MGI) (wt%)	Total acid content (MAA + GA) (wt%)	Methacrylic acid (MAA) (wt%)	Glutaric anhydride (GA) (wt%)	Methyl methacrylate (MMA) (wt%)	Miscibility with SAN 25[c]
IA-250-A	130	1.8	55.7	2.24	1.50	0.74	42.1	Yes
IA-250-B	130	2.0	55.7	2.98	1.94	1.04	41.3	Yes
IA-250-C	131	1.6	55.7	3.26	2.18	1.08	41.0	Yes
IA-250-D	134	1.7	55.7	4.05	2.80	1.25	40.3	Yes
IA-250-E	137	2.1	55.7	7.04	4.64	2.40	37.3	No
IA-245	143	2.1	74.5	0.53	0.08	0.45	25.0	Yes
IA-267	143	n.t.[d]	76.2	1.60	1.01	0.59	22.2	Yes
IA-268	147	n.t.	75.7	4.42	3.13	1.29	19.9	No[e]
IA-264	152	n.t.	76.0	5.81	4.30	1.51	18.2	No
IA-257	157	2.6	87.1	0.70	0.06	0.64	12.2	Yes
IA-271	157	n.t.	89.5	2.90	1.80	1.10	7.6	No
IA-270	161	n.t.	89.5	4.42	3.13	1.29	6.1	No
IA-269	165	3.1	89.5	6.50	5.40	1.10	4.0	No
GA-92	110	n.t.	0	9.20	0.60	8.60	90.8	Yes

[a] For all the IA polymers, $\bar{M}_w \sim 95\,000$; while for GA-92, $\bar{M}_w = 125\,000$
[b] Brabender torque divided by that of nylon-6 (all at 240°C and 60 rev min^{-1} after 10 min)
[c] Tested primarily at 50/50 composition
[d] Not tested
[e] Tested also at SAN 25/IA-268 compositions of 95/5, 90/10, 80/20 and 20/80

simply as *nylon-6* in what follows. When other nylon-6 homopolymers are used, they will be referred to by their commercial designations. Most of the SAN copolymers in *Table 2* have melt viscosities closely matched to those of the polyamides shown in *Table 1*. Two styrene-based functional materials, SMA 25 and Delpet 980N listed in *Table 2*, will be examined for their usefulness as compatibilizers.

Table 3 shows the composition and miscibility characteristics of a series of imidized acrylic (IA) polymers made available by the Rohm and Haas Co. for use in this study. Recently, Rohm and Haas has commercialized an imidized acrylic polymer of this type under the tradename EXL 4140. The total acid content shown for these polymers is the sum of the methacrylic acid (MAA) and glutaric anhydride (GA) units. The molecular weight ($\bar{M}_w$) of these materials has been estimated to be 95 000. These polymers may be broadly categorized into three groups depending on their imide content. Those in the IA-250 series have imide contents of 55.7 wt%. The next group of four have an imide content between 74.5 and 76.2 wt%, while the final four have an imide content between 87.1 and 89.5 wt%. As expected, the T_g of these pure materials increases with increasing imide content (*Table 3*), and they have significantly higher melt viscosities than either the polyamide or the SAN materials used. The final entry in *Table 3* is a terpolymer of methyl methacrylate/methacrylic acid/glutaric anhydride (GA-92).

For melt rheological characterization, the torque in a Brabender Plasticorder with a 50 ml mixing head and standard rotors was recorded when selected polymers were mixed at 240°C and 60 rev min^{-1}. To assess the miscibility characteristics of the imidized acrylic polymers with the SAN copolymers, 50/50 (in most cases) blends were prepared by melt mixing in the Brabender Plasticorder for 10 min at 60 rev min^{-1} and 240°C. Glass transition behaviour was determined using a Perkin–Elmer DSC-7 equipped with a thermal analysis data station at a heating rate of 20°C min^{-1} with samples weighing 5–15 mg. The glass transition temperatures of all the imidized acrylic polymers are substantially above those of the SAN copolymers. Thus, it was possible to differentiate unambiguously miscible (one T_g) from immiscible (two T_g) mixtures.

Ternary blends for morphological analysis were prepared by the simultaneous extrusion of all components in a Killion single-screw extruder ($L/D = 30$, 2.54 cm diameter) at 240°C using a screw speed of 30 rev min^{-1}. All materials containing nylon were dried in a vacuum oven at 80°C for at least 12 h prior to extrusion. The pelletized extruded material was injection moulded into standard Izod (ASTM D256) bars of 0.318 cm thickness using an Arburg Allrounder screw injection moulding machine.

Thin sections were cryogenically microtomed from Izod bars (usually perpendicular to the flow direction) and then examined by transmission electron microscopy (TEM). For ternary blends, a 2% solution of phosphotungstic acid was used in most cases to stain the polyamide matrix to generate sharp contrast between the different phases[35–39]. For binary blends of SAN and the imidized acrylic polymer, ruthenium tetroxide was used to stain the SAN phase[40–43]. A semi-automatic digital image analysis technique was employed to determine the effective diameters of the dispersed phase from TEM photomicrographs using NIH Image software.

RHEOLOGY

Brabender torque rheometry was utilized to characterize the melt flow behaviour of the individual components (*Tables 1–3*) and to obtain some measure of the grafting reactions that occur during melt blending[17,44–46]. *Figure 3* shows the torque after 10 min of mixing as a function of composition for the various imidized acrylic compatibilizers. Within the IA-250 series, the peak maximum shifts to lower IA content as the total reactive functionality

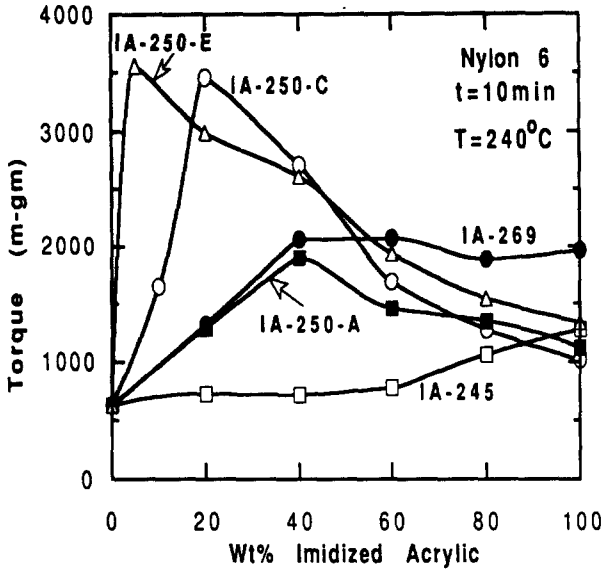

Figure 3 Brabender torque after 10 min at 240°C and 60 rev min^{-1} for nylon-6 blends with selected imidized acrylic polymers

is increased. IA-250-A has the lowest functionality within this series and apparently also displays the least amount of reaction with nylon-6 as manifested by the relatively lower torque levels shown by its blends with nylon-6. In *Figure 3*, IA-245, which has the lowest functionality among these imidized acrylic polymers, shows virtually no indication, by this test, of any reaction with nylon-6. In spite of the relatively high total acid content of IA-269, its blends show much lower torque levels than do blends of either IA-250-C or IA-250-E. This may be attributed to the fact that IA-269 contains a much higher ratio of methacrylic acid groups, which are not as reactive with nylon-6 as anhydride groups[47,48].

MISCIBILITY OF IMIDIZED ACRYLIC POLYMERS WITH STYRENE–ACRYLONITRILE COPOLYMERS

As discussed earlier, miscibility of the imidized acrylic polymers with SAN is an important consideration in their use as a reactive compatibilizer for blends with nylon-6. *Figure 4* summarizes the experimentally determined state of miscibility of each imidized acrylic polymer with a series of SAN copolymers. The results are plotted *versus* the total acid content of the imidized acrylic and AN content of the SAN. The imidized acrylics have been grouped according to their imide content and plotted *versus* their total acid content.

Figure 4a shows that there is a miscibility window for the IA-250 series polymers with SAN copolymers of intermediate acrylonitrile content when the total acid level is ~4% and below. This series has the lowest imide content (55.7 wt%) and displays a relatively large region of miscibility compared to others having higher imide contents (see *Figures 4b* and *4c*). The miscibility zone lies between 20 and 30 wt% AN except for IA-257 (highest imide content), which has a more narrow miscible region. Within each imide content range, miscibility with SAN is lost at high acid levels as described previously[19]. It is clear from these results that, as the imide content increases, miscibility of these materials with SAN tends to be limited to lower acid contents. These observations

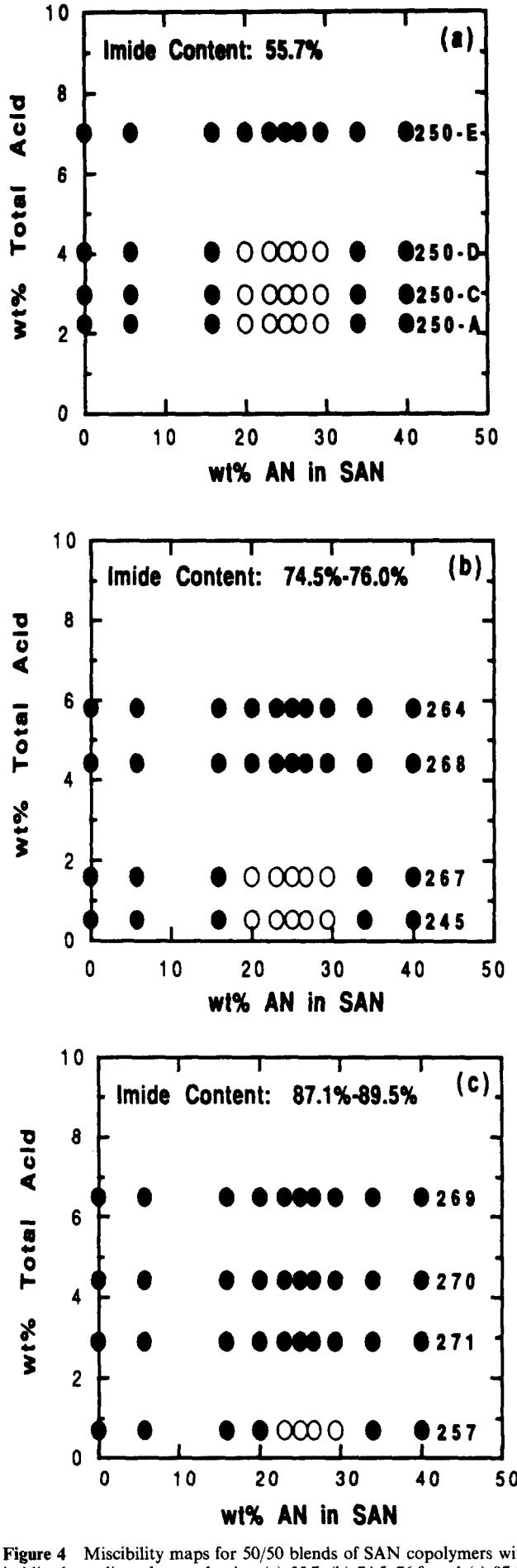

Figure 4 Miscibility maps for 50/50 blends of SAN copolymers with imidized acrylic polymers having (a) 55.7, (b) 74.5–76.0 and (c) 87.1–89.5 wt% imide contents. Open symbols denote miscible blends while full symbols denote immiscible blends

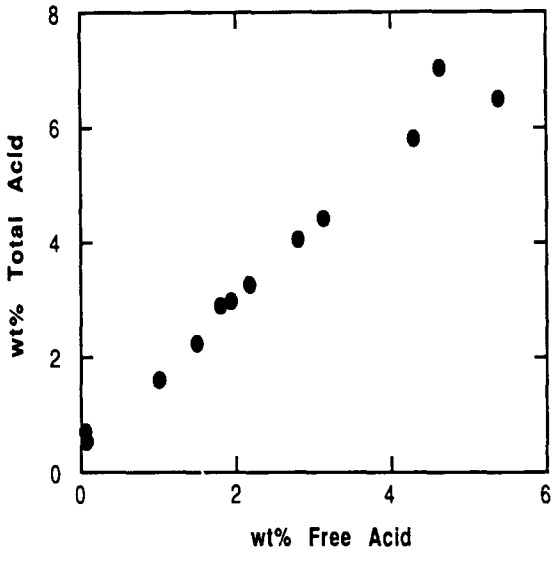

Figure 5 Free acid *versus* total acid content in the imidized acrylic polymers used here

were made primarily for 50/50 blends; however, selected studies at other ratios led to identical conclusions.

The observed phase behaviour for the blends of the imidized acrylic polymers with SAN copolymers reflects the consequence of appropriate summation of all intermolecular and intramolecular interactions in these mixtures[49–51]. Extensive investigations have shown that, over a certain AN range, SAN copolymers are miscible with PMMA[52–60]; on the other hand, it is quite likely that a hypothetical polymer composed of 100% imide units would not be similarly miscible with SAN copolymers. Thus, it is reasonable to expect that increasing the imide content in the imidized acrylic polymers will result in less favourable interactions with SAN copolymers and eventually lead to immiscibility. The fact that acid functionality drives these blends towards immiscibility may stem from the energy needed to break up hydrogen-bonding interactions between the carboxyl groups of the methacrylic acid (MAA) units present in these imidized acrylics.

There is some evidence that the free-acid content is the real factor influencing the miscibility of the imidized acrylics, at fixed imide content, with SAN copolymers. However, the nature of these plots is exactly the same as that shown when the abscissa is changed to the free-acid content of the imidized acrylics. This is a result of the fact that the free-acid and total acid contents are highly correlated within this series, as shown in *Figure 5*.

EFFECT OF IMIDIZED ACRYLIC POLYMERS ON THE MORPHOLOGY OF NYLON-6/STYRENE–ACRYLONITRILE BLENDS

Results for SAN 25

Many ABS materials have a SAN matrix containing approximately 25 wt% AN, so this composition will be the main focus here. *Figure 6* shows TEM photomicrographs for a binary blend of nylon-6 with SAN 25 using two different staining techniques. In *Figure 6a*, the continuous polyamide matrix has been stained with phosphotungstic acid, while in *Figure 6b* ruthenium tetroxide was used to stain the dispersed SAN phase. An average particle size of $\bar{d}_w = 1.4\,\mu m$ was computed for the SAN domain size from these TEM photomicrographs.

Figure 7 shows selected TEM photomicrographs for ternary blends of nylon-6 and SAN 25 containing 5% of the various imidized acrylic polymers from the IA-250 series. In all cases, there is a significant reduction in the SAN domain size compared to the binary blends in *Figure 6*. IA-250-D leads to the smallest particle size within this series, while IA-250-E, which has the highest amount of functionality and is immiscible with SAN 25, leads to a complex morphology consisting of a population of relatively large, irregular and elongated domains ($\bar{d}_w \sim 0.5\,\mu m$) plus a population of much smaller spherical particles ($\bar{d}_w \sim 50\,nm$). *Figure 8* shows the average styrenic phase particle size *versus* the total reactive acid functionality of the added imidized acrylic material. The particle size appears to go through a minimum at approximately 4% total acid functionality (1.25% anhydride) and then increases as the compatibilizer becomes immiscible with the styrenic phase (IA-250-E). The miscible imidized acrylic polymers in this series (A–D) produce regular, spherical particles; whereas, for IA-250-E, which is immiscible with the SAN 25 copolymer used here, the situation is more complex. Although, there is a definite reduction in the average SAN domain size compared to no compatibilizer (*Figure 6*), there seems to be at least two different populations of particles. This morphology and the factors that may be responsible for the

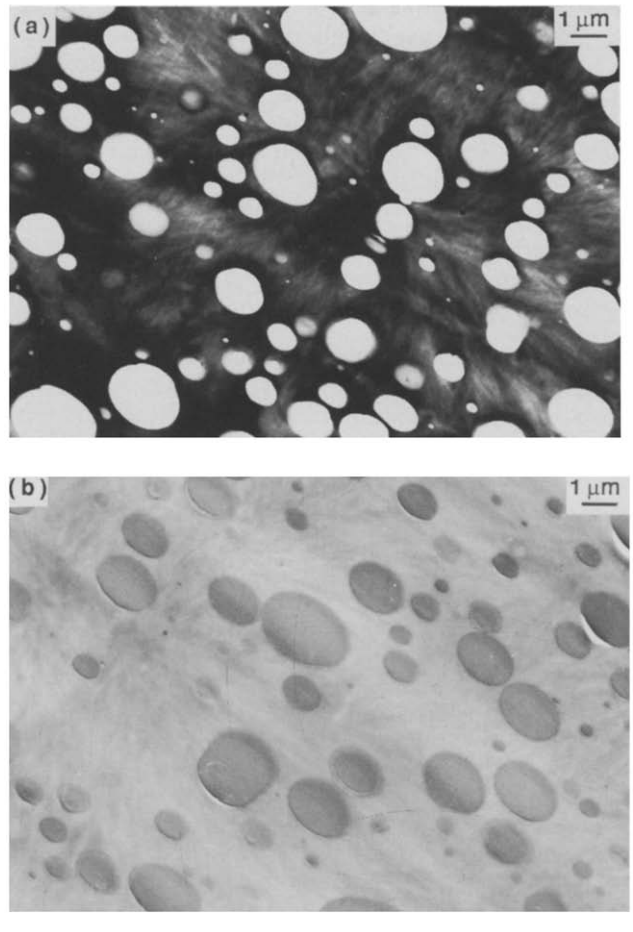

Figure 6 TEM photomicrographs of a nylon 6/SAN 25 (75/25) blend stained (a) with phosphotungstic acid (PTA) and (b) with RuO_4. An average SAN particle size of $\bar{d}_w = 1.4\,\mu m$ was computed from each photomicrograph

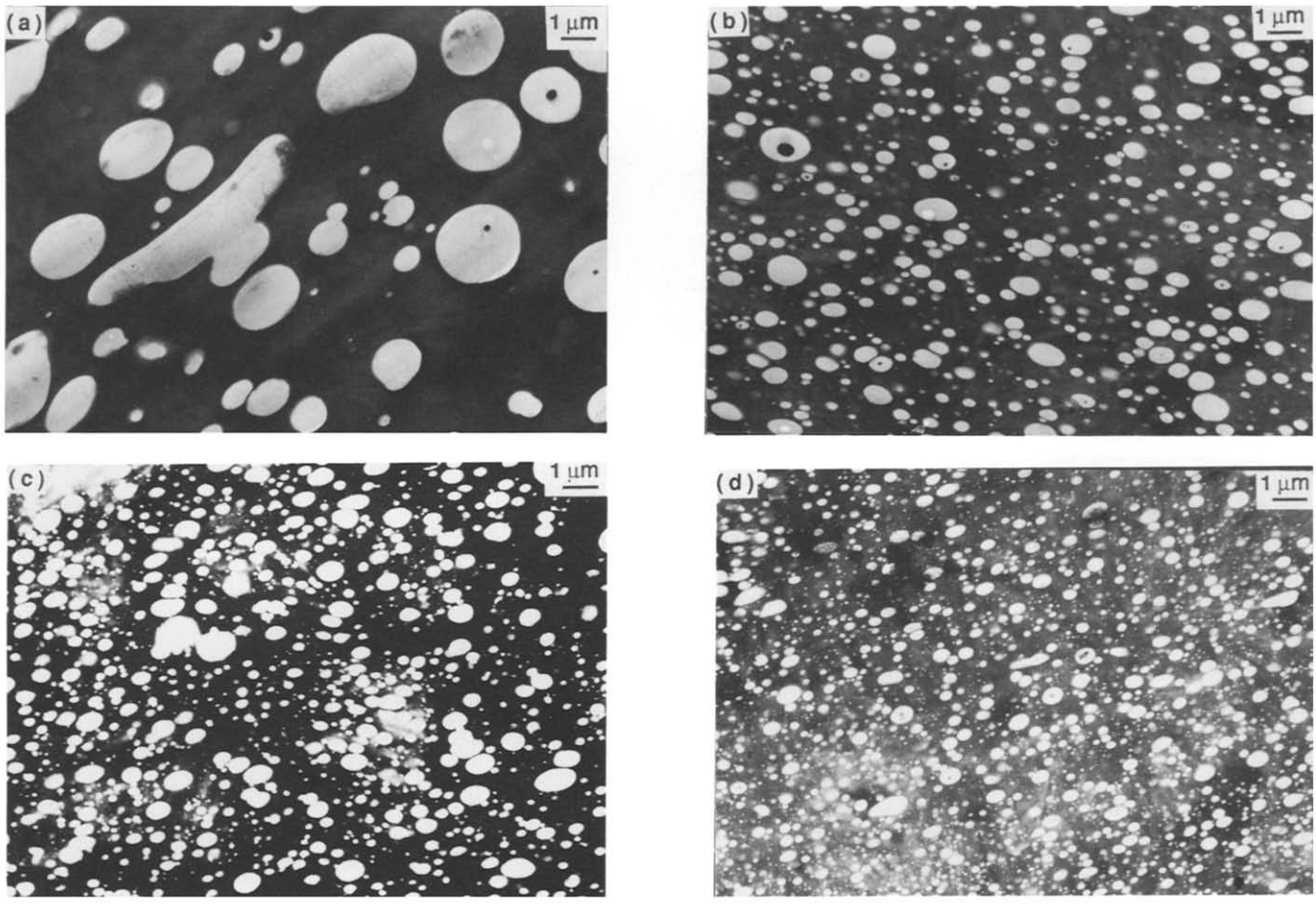

Figure 7 TEM photomicrographs of ternary blends (75/20/5) of nylon-6/SAN 25/imidized acrylic from IA-250 series: (a) IA-250-A, (b) IA-250-C, (c) IA-250-D and (d) IA-250-E. IA-250-A, IA-250-C and IA-250-D are miscible with the SAN phase, while IA-250-E is not. The polyamide phase has been stained with phosphotungstic acid

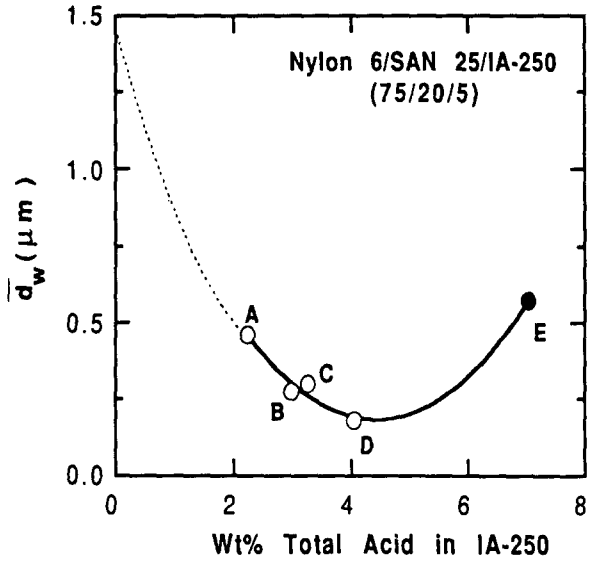

Figure 8 Dispersed-phase domain size in ternary blends (75/20/5) of nylon-6/SAN 25/imidized acrylic as a function of the total acid content of the IA-250 series imidized acrylic polymers. The dotted curve extends to the binary blend of nylon-6/SAN 25 (75/25) where $\bar{d}_w = 1.4\,\mu m$. The open symbols indicate the IA-250 polymers that are miscible with the SAN phase

development of such complex particles will be examined more fully later. Similar morphologies have been observed in our previous work with blends of nylon/SAN using compatibilizers with high levels of anhydride functionality[18].

Figure 9 shows TEM photomicrographs of nylon-6/SAN 25 blends containing 5% of several other imidized acrylic polymers. In *Figures 9a* and *9b* the imidized acrylic compatibilizers are miscible with the SAN phase. The imidized acrylic polymer having the least amount of reactive functionality, IA-245 (*Figure 9a*), produces practically no reduction in the SAN domain size relative to the binary nylon-6/SAN 25 blend. On the other hand, IA-267, which has a relatively higher amount of reactive functionality, reduces the particle size significantly (*Figure 9b*). In *Figures 9c* and *9d*, the imidized acrylic polymers are immiscible with SAN 25, but it is clear that there is a significant reduction in the particle size of the SAN domains in both cases. For IA-268 (*Figure 9d*), the particle size reduction is comparable to that observed with some of the more efficient compatibilizers in the IA-250 series. Interestingly, IA-269 (*Figure 9c*) has a total acid content that nearly matches that of IA-250-E but shows no evidence of the elongated SAN domains observed in the latter case. This may be a consequence of the fact that the major proportion of the total acid functionality in this material is in the free-acid form, i.e. methacrylic acid, which does not react as efficiently with nylon-6 as the anhydride units[47,48] that are more abundant in IA-250-E (see *Figure 3* for a rheological indication of this).

Figure 10 shows the SAN domain size for ternary blends containing 5% of each of the imidized acrylic materials listed in *Table 3* plotted *versus* the total acid content of the imidized acrylic polymer. There is a strong reduction in SAN particle size with increasing total acid

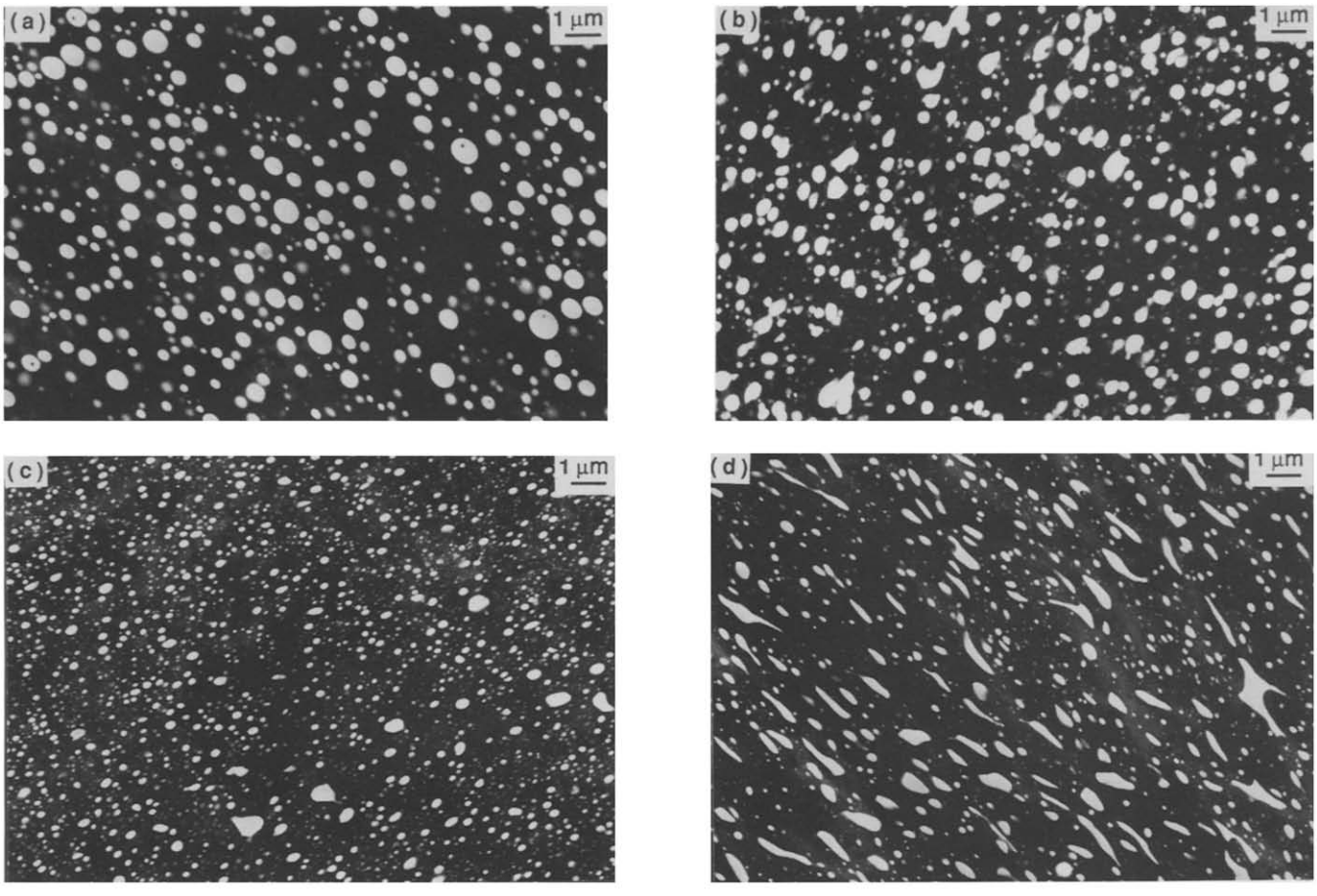

Figure 9 TEM photomicrographs of ternary blends (75/20/5) of nylon-6/SAN 25/imidized acrylic based on (a) IA-245, (b) IA-267, (c) IA-269 and (d) IA-268. IA-245 and IA-267 are miscible with the SAN phase, while IA-269 and IA-268 are not. The polyamide phase has been stained with phosphotungstic acid

content when the imidized acrylic polymer is miscible with SAN 25 (open triangles), while for the imidized acrylic polymers that are not miscible with SAN 25 (full triangles), the average domain size remains fairly constant and somewhat larger. The corresponding plot based on the anhydride content of the imidized acrylic polymer shows similar trends. From these observations, some tentative conclusions can be drawn regarding the optimum structure of the imidized acrylic polymer for the most efficient reduction in SAN domain size.

The ternary polyamide blends prepared using the imidized acrylic polymers that are miscible with the SAN phase are believed to be represented by the model shown in *Figure 2a*. These appear to be the most well behaved systems in that, as the amount of reactive functionality in the imidized acrylic increases, there is a clear reduction in the SAN domain size (*Figures 8* and *10*).

The imidized acrylic polymers that are immiscible with the SAN phase can also produce a considerable reduction in the SAN domain size. The mechanism for this is believed to be best described by the model suggested in *Figure 2b*. This proposal implies that a significant part of the imidized acrylic material is located at the nylon-6/SAN interface through thermodynamic interactions between the phases. This type of wetting should both reduce the effective interfacial tension and cause steric stabilization against coalescence to some degree, with the result being a reduced SAN domain size.

The ternary blends involving IA-250-E are more complicated since distinctly different populations of

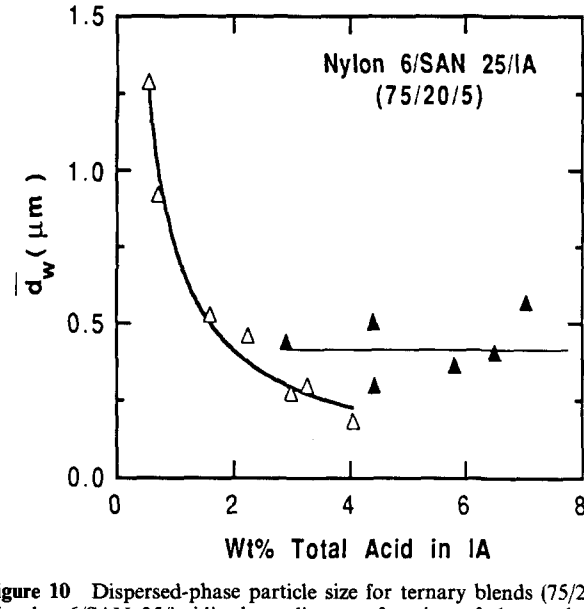

Figure 10 Dispersed-phase particle size for ternary blends (75/20/5) of nylon-6/SAN 25/imidized acrylic as a function of the total acid content of the imidized acrylic polymer. Open symbols denote miscible blends while full symbols denote immiscible blends

particles are evident in the TEM photomicrograph shown in *Figure 7d*. This imidized acrylic polymer is immiscible with SAN 25 but has an exceptionally high amount of anhydride functionality (2.40%). This situation may

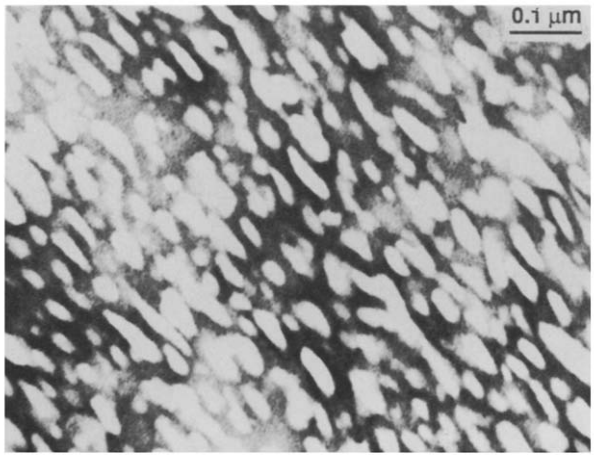

Figure 11 TEM photomicrograph of nylon-6/IA-250-E (75/25) blend. The polyamide phase has been stained with phosphotungstic acid

involve a combination of the models suggested in *Figures 2b* and *2c*. Highly grafted micellar structures like those suggested in *Figure 2c* would be expected to lead to a significantly increased effective melt viscosity of the polyamide matrix, which in turn could be responsible for the type of elongated SAN domains shown in *Figure 7d*. These issues will be explored more fully in a later section.

From the miscibility maps and the particle size data, it appears that the glutarimide and methacrylic acid (MAA) contents influence the miscibility of imidized acrylic polymer with SAN; while SAN domain size and population distribution are primarily influenced by the amount of anhydride groups. Thus, the optimal design of an imidized acrylic polymer for the present purpose is to limit the amount of imide and methacrylic acid groups below a certain level to preserve miscibility with SAN, while maintaining an adequate anhydride concentration for sufficient reaction with the polyamide.

In the screening studies described above, the major phase comprised 75% nylon-6, while the ratio of imidized acrylic polymer to SAN was held constant at 5/20. *Figure 11* shows a highly magnified TEM photomicrograph for the binary blend of nylon-6/IA-250-E (75/25) where the polyamide phase has been stained with phosphotungstic acid. Extremely small domains ($\bar{d}_w = 48$ nm) with a distinct elliptical character are observed as a consequence of the high degree of reaction possible in this system. *Figure 12* shows that the dispersed-phase particle size dramatically changes as the imidized acrylic/SAN 25 ratio is varied across the entire range of concentrations. Going from pure SAN to pure IA-250-C, there is a reduction in particle size by a factor of 30. Similar trends have been shown for other systems[61,62].

Results for other SAN copolymers

The sample TEM photomicrographs in *Figure 13* show how the size of the SAN dispersed-phase particles, with and without the imidized acrylic compatibilizer, IA-250-C, vary with the AN content of the SAN copolymer. For these blends, the viscosity ratio between the polyamide and the styrenic phase has been maintained at approximately unity (*Table 2*). For the uncompatibilized blends, polystyrene gives the largest domains, while the smallest particles are generated in the case of SAN 40. This is believed to stem from the fact that increasing the AN content makes the SAN copolymer more polar and leads to a reduction in the interfacial tension with the polyamide material[18]. Addition of the imidized acrylic polymer leads to a reduction in the particle size in all cases. When polystyrene (PS) is the minor phase, addition of just 5% of the compatibilizer leads to a three-fold reduction in the particle size; while in the case of SAN 20, the domain size is reduced by more than five times. For SAN 40 there is less than a two-fold reduction. It is interesting to note that IA-250-C is miscible with SAN 20 but not with PS or SAN 40.

Figure 14 qualitatively summarizes a broader range of results like those shown pictorially in *Figure 13*. As mentioned above, the steady decrease in particle size with increasing AN content for the binary blends can be attributed to the reduction in the nylon-6/SAN interfacial tension[18] when the SAN/nylon-6 viscosity ratio is held essentially constant. These blends were prepared in a single-screw extruder, and the domain sizes observed are very similar to those prepared in a Brabender Plasticorder[18]. A dramatic reduction in particle size is observed when IA-250-C is added regardless of the AN content of the SAN. The smallest particles are generated in the blends with SAN materials containing 20–30 wt% AN, which corresponds to the IA-250-C/SAN miscibility window shown in *Figure 4a*. Two other compatibilizers, IA-245 and IA-269, were also examined in a similar fashion with the results also shown in *Figure 14*. Addition of IA-245, which has a range of miscibility with SAN copolymers but the lowest degree of functionality of all the imidized acrylic polymers, to the nylon/SAN blends led to a minimal reduction in particle size. On the other hand, addition of IA-269, which is not miscible with any SAN copolymers but has a high degree of total acid functionality, resulted in a significant reduction in the particle size for all the blends shown.

MORPHOLOGY OF BLENDS OF STYRENE–ACRYLONITRILE (SAN 25) AND IMIDIZED ACRYLIC POLYMERS

A carefully selected set of binary blends of imidized acrylic polymers with SAN copolymers was examined by TEM to gain further insights about the interactions involved

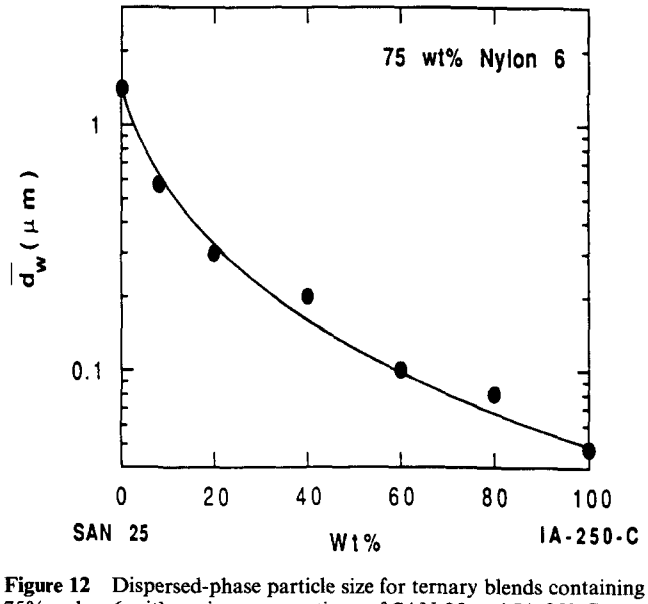

Figure 12 Dispersed-phase particle size for ternary blends containing 75% nylon-6 with various proportions of SAN 25 and IA-250-C

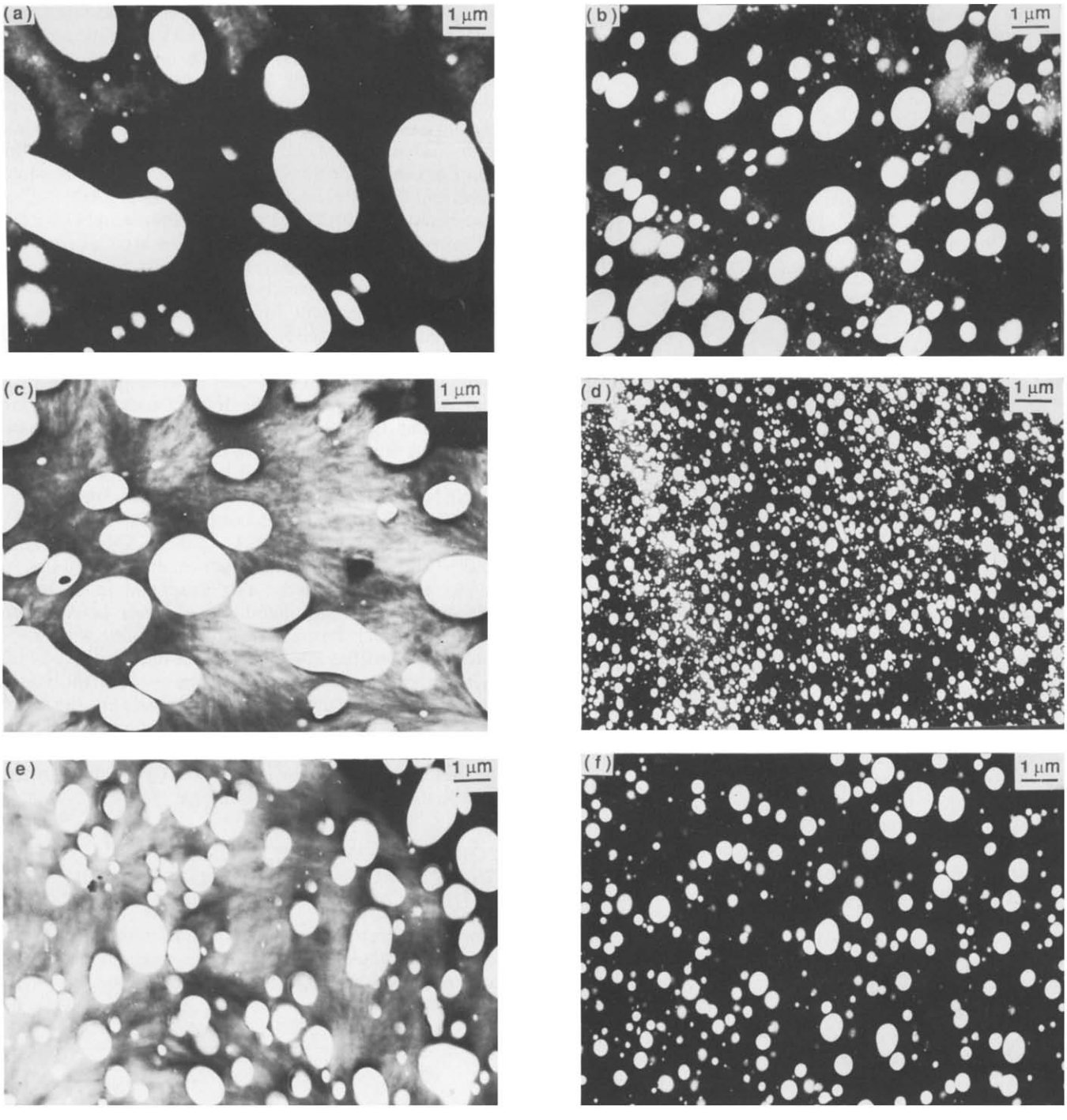

Figure 13 TEM photomicrographs for blends of nylon-6 with three styrenic polymers with and without the IA-250-C imidized acrylic polymer: (a) nylon-6/PS (75/25), (b) nylon-6/PS/IA-250-C (75/20/5); (c) nylon-6/SAN 20 (75/25), (d) nylon-6/SAN 20/IA-250-C (75/20/5); and (e) nylon-6/SAN 40 (75/25), (f) nylon-6/SAN 40/IA-250-C (75/20/5). SAN 20 is miscible with IA-250-C, while PS and SAN 40 are not. The nylon phase has been stained with phosphotungstic acid

in the ternary systems investigated above. Each blend prepared for this analysis contained the same SAN/imidized acrylic ratio (20/5) as in the ternary blends described earlier. Ruthenium tetroxide was used to stain the SAN portion of the thin sections (~50 nm) prepared for TEM analysis.

Figure 15a shows a TEM photomicrograph of a blend of SAN 25 with IA-250-C, which was judged to be miscible by d.s.c. No morphological features other than artifacts are visible, as expected. *Figure 15b* shows a TEM photomicrograph for a binary blend of IA-268 with SAN 25. It may be recalled that, in spite of its apparent immiscibility with SAN 25 by d.s.c., IA-268 is almost as effective as IA-250-C in reducing the SAN domain size in ternary blends with nylon-6 (see *Figures 11* and *12*). Regular, well dispersed domains of the imidized acrylic polymer in the SAN matrix are observed in *Figure 15b*, i.e. two distinct phases, which is consistent with the observation of two T_g values.

The series of imidized acrylics with the highest imide content was used to examine the role of acid functionality on the miscibility and morphological characteristics in

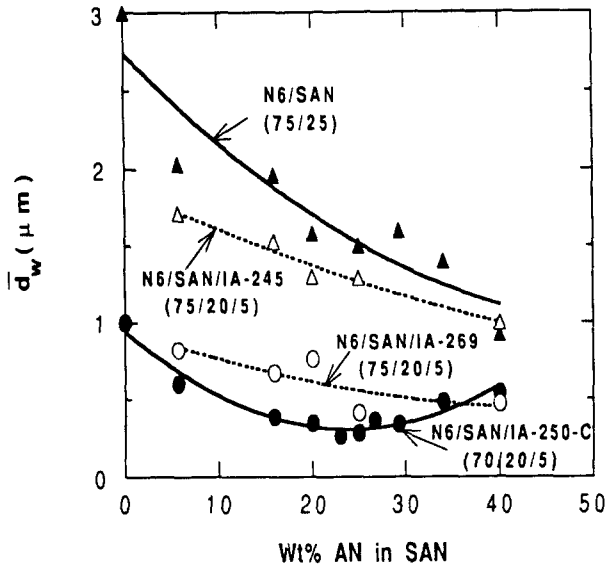

Figure 14 Dispersed-phase particle size for blends of nylon-6 and SAN copolymers (with and without imidized acrylic polymers) as a function of AN content of SAN copolymers

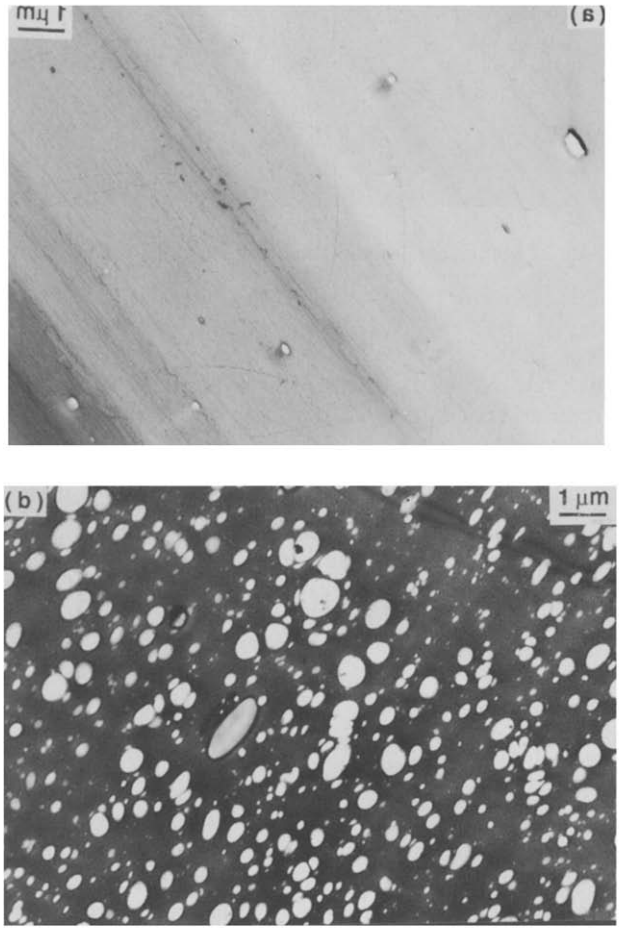

Figure 15 TEM photomicrographs for binary blends (80/20) of (a) SAN 25/IA-250-C (a miscible pair) and (b) SAN 25/IA-268 (an immiscible pair). The SAN phase has been stained with RuO_4

blends with SAN 25. The miscible blend based on IA-257 shows no morphological features on TEM analysis, indicating a homogeneous phase consistent with the single T_g (*Figure 4c*) observed for these blends. As the acid functionality is increased, the imidized acrylic material distinctly shows up as the dispersed phase, which progressively becomes larger in size. *Figure 16* shows the size of the imidized acrylic polymer particles formed in blends with SAN 25 as a function of the methacrylic acid (MAA) content. Increased methacrylic acid content leads to stronger cohesive forces in these imidized acrylic polymers via hydrogen bonding of the carboxylic groups. The relationship shown in *Figure 16* no doubt reflects an increase in the interfacial tension between the two phases as the free-acid content in the imidized acrylic polymer increases[8,9].

NYLON-6/STYRENE–ACRYLONITRILE BLENDS CONTAINING HIGHLY FUNCTIONAL COMPATIBILIZERS

Various factors were briefly mentioned earlier that may lead to the irregular morphology observed in the ternary blends containing the highly functional IA-250-E. The morphology of this ternary blend is examined in greater detail here along with similar blends containing other compatibilizers with a high degree of reactive functionality, namely GA-92, SMA 25 and Delpet 980N, as described in *Tables 2* and *3*.

Figure 17 compares TEM photomicrographs of ternary blends based on these four materials. Each photomicrograph is at the same magnification and the polyamide matrix was stained with phosphotungstic acid. In each case, three types of dispersed-phase particles can be identified and classified as: (a) relatively large and elongated particles of complex shapes that tend towards co-continuity with the polyamide phase; (b) smaller, somewhat irregular but predominantly elliptical particles having an effective diameter between 0.5 and 1.0 μm; and (c) extremely small, round particles that are less than 50 nm in size. The morphologies of the blends based on IA-250-E and GA-92 shown in *Figures 17a* and *17b* are very similar. For the blends based on SMA 25 (*Figure 17c*), the elongated domains appear to be significantly broader, which may be related to its extremely high level

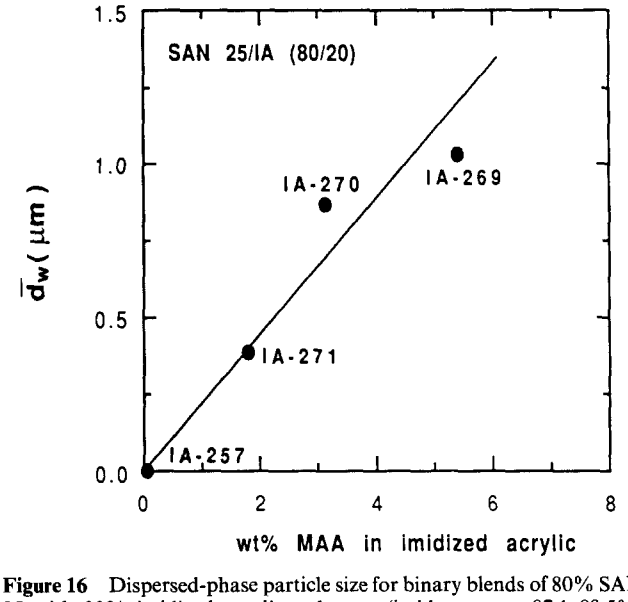

Figure 16 Dispersed-phase particle size for binary blends of 80% SAN 25 with 20% imidized acrylic polymers (imide content 87.1–89.5%) *versus* methacrylic acid (MAA) content of the imidized acrylic. For the miscible binary blend with IA-257, $\bar{d}_w$ has been set equal to zero

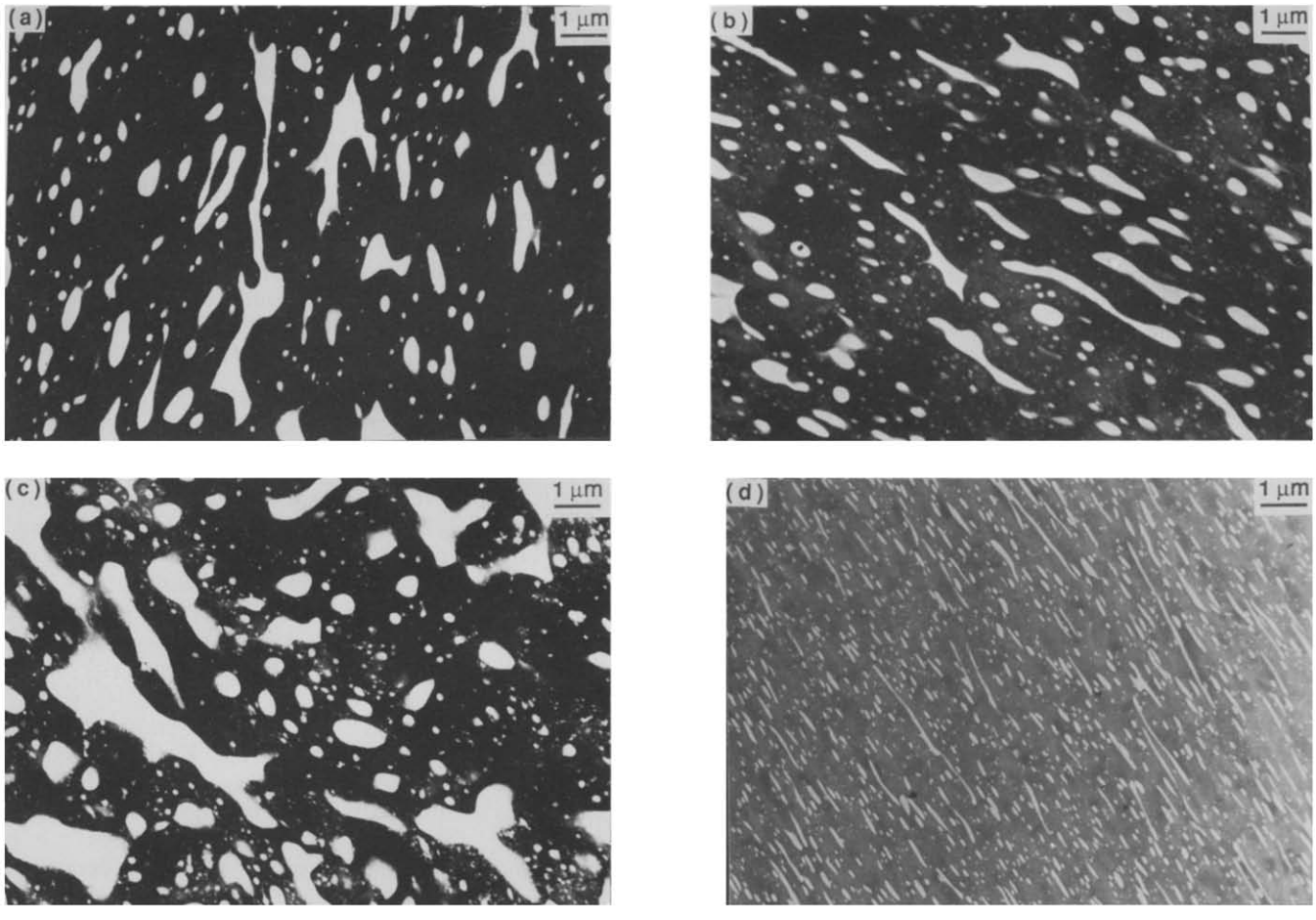

Figure 17 TEM photomicrographs for ternary (75/20/5) nylon-6 blends with SAN 25 and imidized acrylic containing 5% (a) IA-250-E, (b) GA-92, (c) SMA 25, and (d) Delpet 980N

of reactive functionality. In the case of Delpet 980N (*Figure 17d*), the elongated domains appear to be somewhat more stringy in nature. These photomicrographs show morphological features similar to those observed in an earlier study of nylon/SAN blends, containing highly functionalized styrenic compatibilizers, prepared in a Brabender Plasticorder and examined by less revealing SEM techniques[18].

Detailed TEM analysis of ternary blends based on IA-250-E

All of the photomicrographs shown earlier were for sections microtomed from Izod bars perpendicular to the flow direction. Such two-dimensional views can only yield limited information about the overall three-dimensional morphology in complex systems. Therefore, a more detailed characterization of nylon-6/SAN 26/IA-250-E blends was made. *Figure 18a* defines the three orthogonal planes of an Izod bar from which sections were microtomed near its centre. According to this convention, all of the TEM photomicrographs shown earlier were taken from the 2–3 plane, i.e. perpendicular to the flow direction. *Figures 18b* and *18c* show TEM photomicrographs obtained from the 1–2 and 1–3 planes, respectively. A careful comparison reveals some subtle differences between planes. Compared to the 2–3 plane (*Figure 17a*), the elongated particles in the 1–2 plane appear to be oriented in a preferred direction (*Figure 18b*). In addition to the three distinct populations of particles observed in the other two orthogonal directions, several irregular, broad domains are also evident in the 1–3 plane (*Figure 18c*).

From this series of TEM photomicrographs, it seems reasonable to conclude that the elongated structures observed in the 2–3 and the 1–2 planes (in *Figures 18b* and *18c*) are actually side views of complex platelet-like domains of SAN. This proposal is supported by the several broad structures observed in the 1–3 plane. The small, regular particles ($\bar{d}_w \sim 50$ nm) seen in all three orthogonal planes confirm the existence of a very significant population of extremely small, nearly spherical domains in this blend.

It is tempting to propose that the larger, complex particles as well as the elliptical particles of intermediate size observed in *Figures 17a*, *18b* and *18c* are primarily SAN-rich domains and that the smallest population of particles are nylon-grafted micellar aggregates of the imidized acrylic material as expected from the model in *Figure 2c*. Note that SAN 25 and IA-250-E are judged to be immiscible by d.s.c. This hypothesis is briefly examined here using a different staining technique. Ruthenium tetroxide should stain the SAN in these ternary blends (see *Figure 6b*), leaving the imidized acrylic polymer virtually unstained (*Figures 11* and *15b*) if these exist as distinct entities.

Figures 19a and *19b* show TEM photomicrographs of sections from the 2–3 and 1–2 planes of an Izod bar, respectively, stained with ruthenium tetroxide. *Figure 19c*

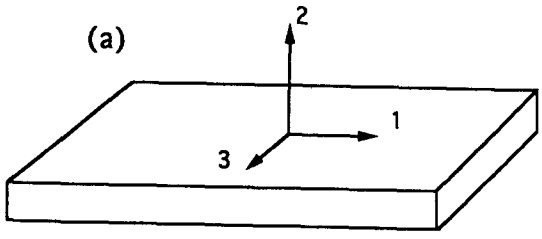

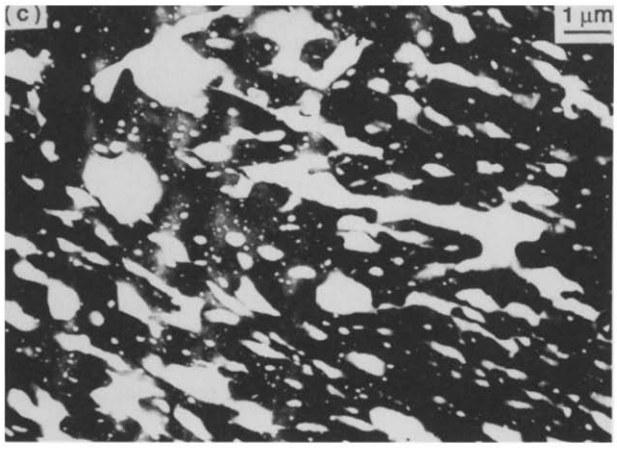

Figure 18 (a) Various planes in an Izod bar from which ultramicrotomed sections were obtained for TEM analysis. TEM photomicrographs of sections microtomed from (b) the 1–2 plane and (c) the 1–3 plane of an Izod bar made from the ternary polyamide blend (75/20/5 nylon-6/SAN 25/IA-250-E). The polyamide phase has been stained with phosphotungstic acid

shows a view of the same blend from the 2–3 plane at a much higher magnification. In all three of these photomicrographs, the same three distinct populations of particles described earlier are observed. Even the smallest particles ($\bar{d}_w = 50$–100 nm) are stained by ruthenium tetroxide. We believe that these smallest particles are imidized-acrylic-rich domains that contain enough SAN to make them susceptible to staining by ruthenium tetroxide. Only a small amount of SAN ($\sim 5\%$) would be required. The presence of SAN might be attributed either to a small amount of pre-existing partial miscibility between the IA-250-E and SAN 25 (not detected by cursory d.s.c. analysis) or to the generation of such a state of miscibility during the course of blend preparation through modification of the molecular structure of the imidized acrylic. The latter could result from reaction of the free-acid groups (which induce immiscibility) to form anhydrides (through reaction with a neighbouring methacrylate group with the evolution of methanol) or imide groups (through reaction with the nylon-6 material). In principle, such reactions could lead to more favourable thermodynamic interactions that would result in a certain amount of partial miscibility of SAN in the imidized acrylic domains.

Proposed mechanism for generation of complex morphologies with highly functional compatibilizers

No doubt many factors may contribute to the complex morphology observed above. However, the following

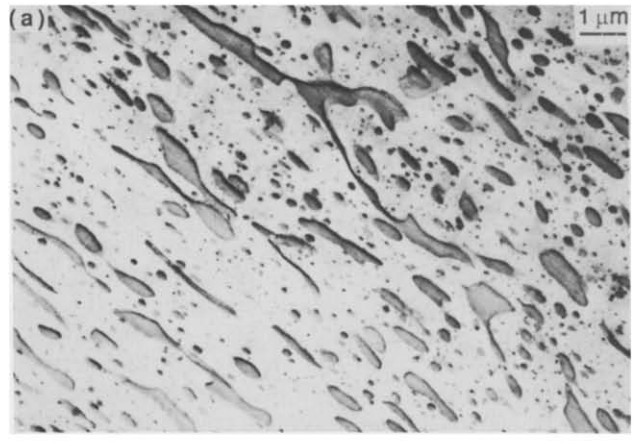

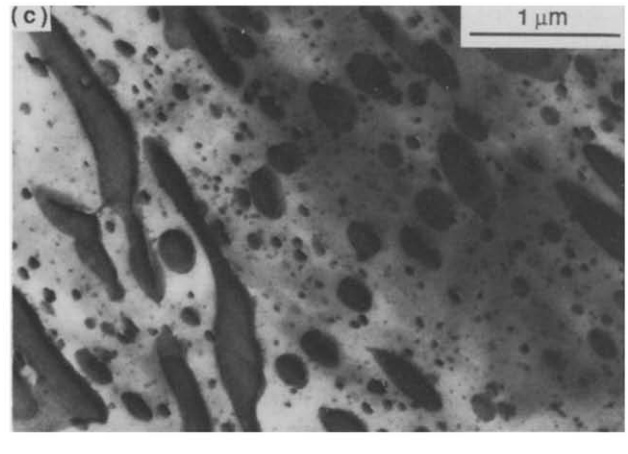

Figure 19 TEM photomicrographs of sections from the ternary polyamide blend (75/20/5 nylon-6/SAN 25/IA-250-E) obtained from (a) the 2–3 plane, (b) the 1–2 plane and (c) the 2–3 plane of an Izod bar. RuO_4 has been used as a staining agent. The TEM photomicrograph in (c) is at a higher magnification using the same staining technique

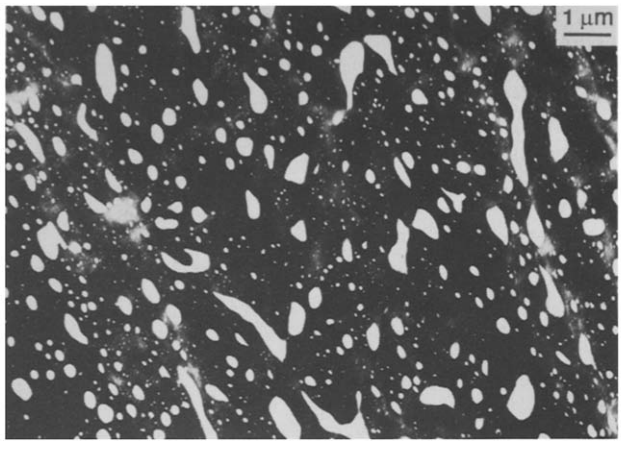

Figure 20 TEM photomicrograph from the 2–3 plane of the ternary polyamide blend (75/20/5 B5/SAN 25/IA-250-C). The polyamide phase has been stained with phosphotungstic acid

proposal seems to explain all the essential features. The most plausible mechanism, in our view, for the formation of the large platelet or stringy domains described above involves changes in the relative melt rheological characteristics of the phases caused by the *in situ* reaction. The microscopy described earlier suggests that the very tiny dispersed particles consist of a phase of reactive imidized acrylic polymers to which nylon-6 chains are grafted to form micellar-like structures. The polyamide phase modified in this way will have a substantially increased melt viscosity[63–65] as, in fact, can be seen in *Figure 3*. As the polyamide (plus grafted micellar particles) phase becomes much more viscous than the large, dispersed particles (believed to consist mainly of SAN material), these particles will have a tendency to become co-continuous even though they form the minor phase[66–69]. This tendency leads to the formation of stringy or platelet structures when conditions are not sufficient to convert them into a continuous phase.

This effect can be simulated by use of a high-molecular-weight nylon-6 material, B5, as the matrix in a ternary blend with SAN and an imidized acrylic polymer with a much lower reactive functionality, viz. IA-250-C (see *Table 3* for composition). The B5 nylon-6 has a significantly higher melt viscosity at corresponding shear rates (see Brabender data in *Table 1*) than the standard nylon-6 used in the above discussion. A TEM photomicrograph of the ternary blend based on this high-molecular-weight nylon-6 and the low-functionality imidized acrylic (see *Figure 20*) reveals striking similarities to those in *Figures 17–19*. It is important to note that the SAN blends based on the lower-viscosity nylon-6 (Capron 8207F) employing the same compatibilizer used in prior experiments contains only spherical particles (see *Figure 7b*). These observations clearly demonstrate that an increased viscosity of the polyamide matrix may indeed lead to irregular shapes of the styrenic phase like those discussed earlier.

It is relatively simple to visualize the formation of two dispersed phases consisting of extremely small grafted micellar aggregates and larger complex particles in these ternary blends when the imidized acrylic polymer (IA-250-E in the above example) is not miscible with SAN 25. However, it is somewhat more difficult to rationalize the formation of such structures in the case of GA-92, Delpet 980N and SMA 25 since they are miscible with SAN 25. Why should a certain proportion of the compatibilizer material phase-segregate from the SAN 25 copolymer and form micellar aggregates in the polyamide matrix? One possibility is that the reactions occurring during the reactive extrusion process alter the molecular composition of these compatibilizers to an extent that they become immiscible with the SAN phase. For example, if a significant fraction of the anhydride groups are converted into imides by reaction with the polyamide, it is quite possible that the reacted compatibilizer could become immiscible with the SAN phase. A second possibility is that rheological stresses transmitted to the compatibilizer molecule by multiple nylon grafts could mechanically rip the graft copolymer from the interfacial region and form micellar domains in the polyamide matrix (as suggested by the model in *Figure 2c*). In fact, these two possibilities could act together. In any case, the proposal outlined here requires some mechanism to increase the viscosity of the polyamide phase, which in turn causes the SAN domains to tend to become co-continuous with the nylon phase when the compatibilizer has high levels of functionality.

Other processes that tend to promote this type of morphology can also be envisioned. For example, a high density of comb-like graft copolymer at the interface between the continuous and dispersed phases might create either bulk or interfacial elasticity that would strongly impede the rate of drop break-up[70,71] and could potentially lead to the formation of elongated domains with a marked tendency towards co-continuity (as seen in *Figures 17–19*).

Clearly, the combination of physical and chemical events involved in the morphology generation in such reactive blends is very complex, and it is indeed difficult to resolve unambiguously all the issues that might be important. This would be an extremely fruitful area for detailed studies on model systems that isolate specific mechanisms and the interdependences suggested above.

EFFECT OF POLYAMIDE CHEMISTRY ON MORPHOLOGY

Finally, it is appropriate to explore the effect of some of the chemical characteristics of the polyamide matrix on the morphology of these blends with SAN 25 and the imidized acrylic polymer, IA-250-C. In particular, nylon-6,6 and its copolymers with nylon-6 are examined. As explained previously[61,62], nylon-6,6 has a certain fraction of chains with amine groups at both ends and, therefore, is difunctional in terms of its reactions with phases containing anhydride or acid groups. This can have dramatic effects on phase morphology as demonstrated previously[61,62,72]. Copolymers of nylon-6 with nylon-6,6, if random in structure and if the nylon-6,6 monomers are present in precisely stoichiometric amounts, ought to have a fraction of chains with diamine functionality that is in proportion to their nylon-6,6 content. A nylon-6 with enriched amine chain ends (some chains have amine groups at both ends) was also used. *Figure 21a* shows a TEM photomicrograph for a binary blend of nylon-6,6/SAN 25. The SAN domains are about the same size as those in comparable blends with nylon-6, since the two polyamides should have similar interfacial tension with SAN 25 and were chosen to have the same melt viscosity. Addition of IA-250-C leads to reduction in the

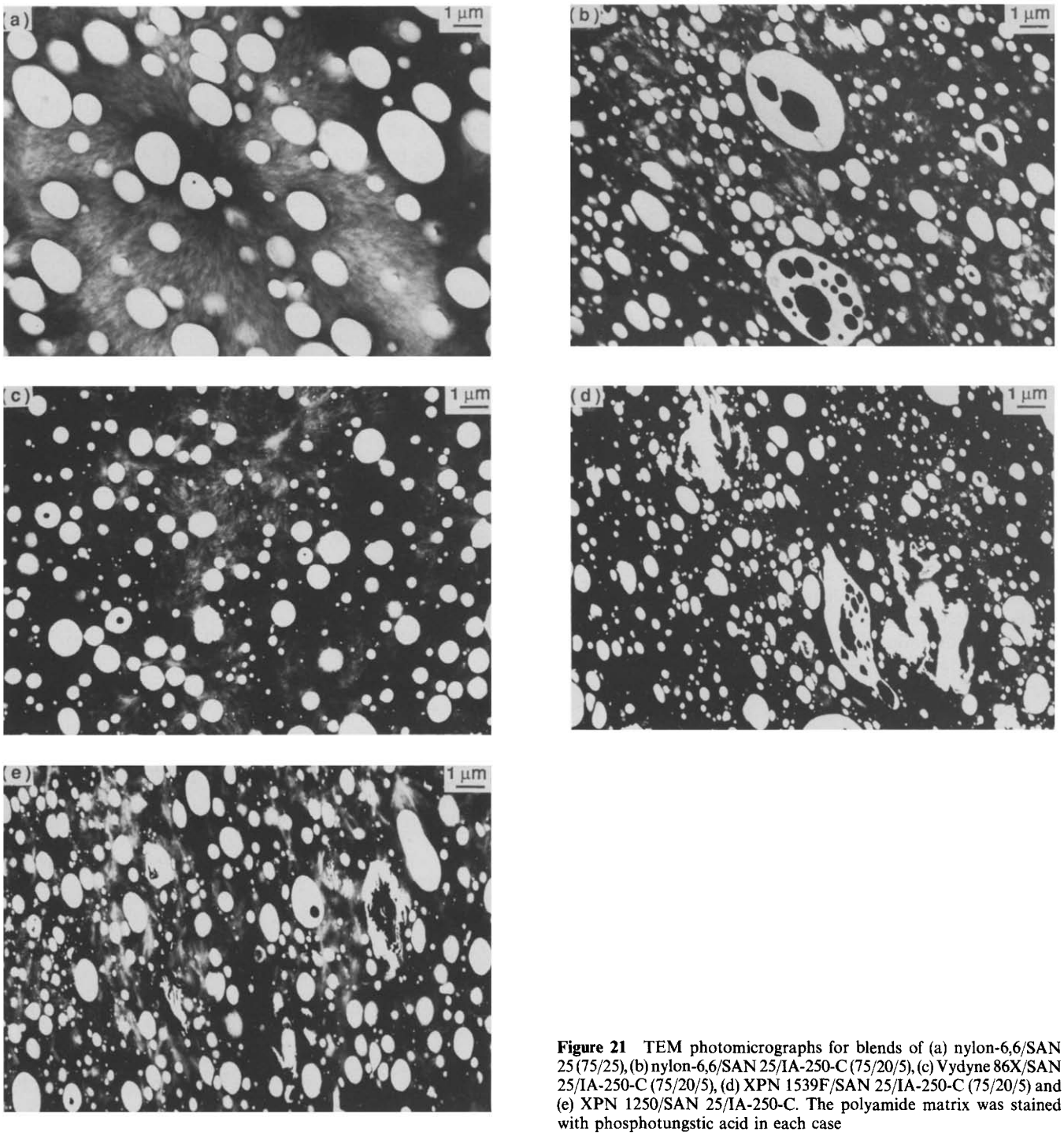

Figure 21 TEM photomicrographs for blends of (a) nylon-6,6/SAN 25 (75/25), (b) nylon-6,6/SAN 25/IA-250-C (75/20/5), (c) Vydyne 86X/SAN 25/IA-250-C (75/20/5), (d) XPN 1539F/SAN 25/IA-250-C (75/20/5) and (e) XPN 1250/SAN 25/IA-250-C. The polyamide matrix was stained with phosphotungstic acid in each case

size of some of the particles as shown in *Figure 21b*; however, several extremely large SAN particles with polyamide material occluded inside them are also present. *Figures 21c* and *21d* show TEM photomicrographs of ternary blends based on the copolymers of nylon-6 and nylon-6,6. While there is further reduction in the SAN domain size using Vydyne 86X (a copolymer containing 16% nylon-6) as the polyamide matrix, a combination of spherical and extremely complex particles are present when the polyamide copolymer XPN 1539F (85% nylon-6) forms the matrix. *Figure 21e* shows the TEM photomicrograph of the ternary blend based on the amine-terminated nylon (XPN 1250). While there is some evidence of complex SAN domains in this case, the majority of the particles appear to be spherical and regular in shape ($\bar{d}_w = 0.91\ \mu m$).

Figure 22 shows a steady reduction in SAN particle size as the proportion of nylon-6 increases in the polyamide matrix material. The smallest particles are formed in the nylon-6 homopolymer, where only a single end-grafting mechanism is possible. This is optimum for reducing the particle size via lowering interfacial tension and for stabilizing the SAN domains against coalescence[61,72]. Nylon-6,6, on the other hand, produces the largest particles, which no doubt stem from the two end-grafting mechanisms that are possible for those chains having two amine end-groups[61,62,72]. The extremely complex particles present in the case of the nylon-6/nylon-6,6 copolymer (XPN 1539F) and to some extent in the amine-terminated nylon (XPN 1250) may be attributed to the loops and particle bridges that are possible in polyamides with some degree of difunctionality[61,72]. No

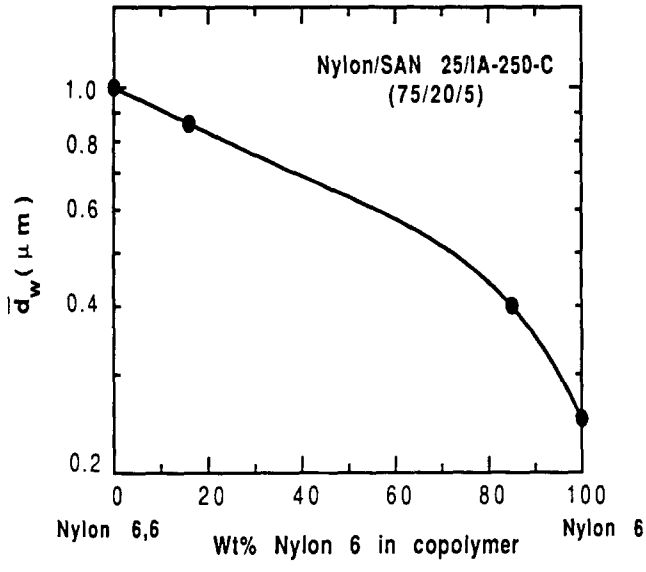

Figure 22 Effect of nylon-6,6 content of polyamide copolymers on dispersed-phase particle size of ternary blends (75/20/5) of polyamide/SAN 25/IA-250-C

doubt a finer degree of dispersion could be achieved by using devices such as a co-rotating, fully intermeshing twin-screw extruder that provide more intensive mixing than the single-screw extruder employed here.

CONCLUSIONS

Addition of reactive polymers to the SAN phase of ABS materials has been repeatedly shown[11–17] to be an effective strategy for controlling morphology and producing super-tough nylon/ABS blends. A model system, in which the rubber phase in the ABS was omitted for reasons of simplicity, was explored here to gain insights about the generation of morphology in nylon/SAN blends using compatibilizers with anhydride and/or acid functionalities. The main thrust was to evaluate a series of imidized acrylic polymers as reactive compatibilizers.

The miscibility characteristics of each imidized acrylic polymer with the SAN phase and the level of reactive functionality were shown to have strong influences on the morphology generated in nylon-6/SAN systems. In general, low methacrylic acid and imide contents favour miscibility of imidized acrylic polymers with SAN; while the amount of anhydride present in these compatibilizers strongly affects the reactivity and consequently the morphology (dispersed-phase domain size and shape) generated in ternary polyamide blends. The most efficient size reduction in the dispersed-phase particle size occurs when the compatibilizer is miscible with the SAN phase and has an optimum amount of anhydride functionality (as suggested by the simple model shown in *Figure 2a*). Imidized acrylic compatibilizers that are not miscible with the SAN phase but have sufficient reactive functionality also lead to some reduction in the SAN dispersed-phase particle size. This can be rationalized to an extent via the model shown in *Figure 2b*. Higher anhydride functionality in the imidized acrylic polymer (and in other compatibilizers like GA-92, SMA 25, Delpet 980N) than an optimum level leads to a more complex morphology for these ternary polyamide blends (*Figures 17–19*). These situations are believed to stem from full or partial segregation of the SAN and compatibilizer into separate dispersed domains. An increase in the viscosity of the polyamide/compatibilizer matrix can cause the SAN-rich phase to enlarge and tend towards co-continuity.

The functional character of the polyamide matrix influences the size and shape of SAN domains generated in the compatibilized blends. In general, increasing the difunctional character of the polyamide (more nylon-6,6 units or amine-terminated nylon-6) leads to larger SAN domains. This is believed to be a result of two end-grafting mechanisms that are possible for some of the polyamide chains[61,62,72].

Future papers will relate the observations and conclusions reached here for these simple ternary systems to the morphology and mechanical properties of the more complex and commercially attractive nylon/ABS blends.

ACKNOWLEDGEMENTS

This research was supported by the US Army Research Office. The authors are indebted to the Rohm and Haas Co. for the various compatibilizer materials and to Daniel Kallick of the Photography Department at the University of Texas at Austin.

REFERENCES

1 Teyssie, P. *Makromol. Chem., Macromol. Symp.* 1988, **22**, 83
2 Sjoerdsma, S. D., Bleijenberg, A. C. A. M. and Heikens, D. *Polymer* 1981, **22**, 619
3 Paul, D. R. in 'Functional Polymers' (Eds D. E. Bergbreiter and C. E. Martin), Plenum Press, New York, 1989, p. 1
4 Paul, D. R., Barlow, J. W. and Keskkula, H. in 'Encyclopedia of Polymer Science and Engineering' (Eds Mark, Bikales, Overberger and Menges), Wiley-Interscience, New York, 2nd Edn, 1988, Vol. 12, p. 399
5 Paul, D. R. in 'Thermoplastic Elastomers: Research and Development' (Eds N. R. Legge, H. Schroeder and G. Holden), Hanser Verlag, Munich, 1987, Ch. 12, Sec. 6
6 Willis, J. M. and Favis, B. D. *Polym. Eng. Sci.* 1988, **28**, 1416
7 Favis, B. D. and Chalifoux, J. P. *Polym. Eng. Sci.* 1987, **27**, 1591
8 Wu, S. *Polym. Eng. Sci.* 1987, **27**, 335
9 Serpe, G., Jarrin, J. and Dawans, F. *Polym. Eng. Sci.* 1990, **30**, 553
10 Park, I., Keskkula, H. and Paul, D. R. *J. Appl. Polym. Sci.* 1992, **45**, 1313
11 Lavengood, R. E. and Silver, F. M. *SPE Tech. Papers* 1987, **33**, 1369
12 Lavengood, R. E., Patel, R. and Padwa, A. R., US Pat. 4777211 (Monsanto), 1988
13 Lavengood, R. E., Padwa, A. R. and Harris, A. F., US Pat. 4713415 (Monsanto), 1987
14 Aoki, Y. and Watanabe, M., US Pat. 4987185 (Monsanto Kasei Co.), 1991
15 Howe, D. V. and Wolkowicz, M. D. *Polym. Eng. Sci.* 1987, **27**, 1582
16 Padwa, A. R. and Lavengood, R. E. *ACS Symp. Ser.* 1992, **33**, 600
17 Triacca, V. J., Ziaee, S., Barlow, J. W., Keskkula, H. and Paul, D. R. *Polymer* 1991, **32**, 1401
18 Takeda, Y. and Paul, D. R. *J. Polym. Sci. (B) Polym. Phys.* 1992, **30**, 1273
19 Fowler, M. E., Paul, D. R., Cohen, L. A. and Freed, W. T. *J. Appl. Polym. Sci.* 1989, **37**, 513
20 Graves, G., US Pat. 2146209 (Du Pont), 1939
21 Schroeder, G., US Pat. 3284425 (Rohm GmbH), 1966
22 Gotzen, F., Schroeder, G. and Schulz, G. V. *Makromol. Chem.* 1965, **88**, 133
23 Ganzler, V. W., Huch, P., Metzger, W. and Schroeder, G. *Angew. Makromol. Chem.* 1970, **11**, 91
24 Butler, G. B. and Myers, G. R. *J. Macromol. Sci. Chem.* 1971, **1**, 105
25 Kopchik, R. M., US Pat. 4246374 (Rohm and Haas), 1981
26 Hallden-Abberton, M., Bortnik, N., Chen, L., Freed, W. and Fromuth, H. US Pat. 4954574 (Rohm and Haas), 1990

27 Hallden-Abberton, M. *Polym. Mater. Sci. Eng.* 1991, **65**, 361
28 Hallden-Abberton, M., Cohen, L. and Wood, R., US Pat. 4874824 (Rohm and Haas), 1989
29 Hallden-Abberton, M., Bortnick, N., Cohen, L., Freed, W. and Fromuth, H., US Pat. 4727117 (Rohm and Haas), 1988
30 Kopchik, R. M., US Pat. 4255322 (Rohm and Haas), 1981
31 Staas, W., US Pat. 4415706 (Rohm and Haas), 1983
32 Staas, W., US Pat. 4436871 (Rohm and Haas), 1984
33 Kopchik, R. M., US Pat. 4742123 (Rohm and Haas), 1988
34 Hallden-Abberton, M., US Pat. 5084517 (Rohm and Haas), 1992
35 Martinez-Salazar, J. and Cannon, C. G. *J. Mater. Sci. Lett.* 1984, **3**, 693
36 Morel, D. E. and Grubb, D. T. *Polymer* 1984, **25**, 41
37 Boylston, E. K. and Rollins, M. L. *Microscope* 1971, **19**, 255
38 Spit, B. J. *Faserforsch. Textiltech.* 1967, **18**, 161
39 Rusnock, J. A. and Hansen, D. *J. Polym. Sci.* (*A*) 1965, **3**, 617
40 Trent, J. S. *Macromolecules* 1984, **17**, 2930
41 Trent, J. S., Scheinbeim, J. I. and Couchman, P. R. *Macromolecules* 1983, **16**, 589
42 Trent, J. S., Scheinbeim, J. I. and Couchman, P. R. *J. Polym. Sci., Polym. Lett. Edn* 1981, **19**, 315
43 Vitali, R. and Montani, E. *Polymer* 1980, **21**, 1220
44 Barlow, J. W., Shaver, G. P. and Paul, D. R. Proc. First Int. Congr. on Compatibilization and Reactive Polymer Alloying (Compalloy '89), New Orleans, LA, 1989, p. 221
45 Fowler, M. W. and Baker, W. E. *Polym. Eng. Sci.* 1988, **28**, 1427
46 Baker, W. E. and Saleem, M. *Polymer* 1987, **28**, 2057
47 Lu, M., Keskkula, H. and Paul, D. R. *Polymer* 1993, **34**, 1874
48 Lu, M., Keskkula, H. and Paul, D. R. *Polym. Eng. Sci.* 1994, **34**, 33
49 Paul, D. R. and Barlow, J. W. *Polymer* 1984, **25**, 487
50 ten Brinke, G., Karasz, F. E. and MacKnight, W. J. *Macromolecules* 1983, **16**, 1827
51 Kambour, R. P., Bendler, J. T. and Bopp, R. C. *Macromolecules* 1983, **16**, 753
52 Fowler, M. E., Barlow, J. W. and Paul, D. R. *Polymer* 1987, **28**, 1177
53 Nishimoto, M., Keskkula, H. and Paul, D. R. *Polymer* 1989, **30**, 1279
54 Kressler, J., Kammer. H. W. and Klostermann, K. *Polym. Bull.* 1986, **15**, 113
55 Suess, M., Kressler, J., Kammer, H. W. and Heinemann, K. *Polym. Bull.* 1986, **16**, 371
56 Sanchez, I. C. *Polymer* 1989, **30**, 471
57 Stein, D. J., Jung, R. H., Iller, K. H. and Hendus, H. *Angew. Makromol. Chem.* 1974, **36**, 89
58 Naito, K., Johnson, G. E., Allara, K. L. and Kwei, T. K. *Macromolecules* 1978, **11**, 1260
59 Chiou, J. S., Paul, D. R. and Barlow, J. W. *Polymer* 1982, **23**, 1543
60 Bernstein, R. E., Cruz, C. A. and Paul, D. R. *Macromolecules* 1977, **10**, 681
61 Oshinski, A. J., Keskkula, H. and Paul, D. R. *Polymer* 1992, **33**, 268 and 284
62 Takeda, Y., Keskkula, H. and Paul, D. R. *Polymer* 1992, **33**, 3173
63 Utracki, L. A. and Sammut, P. *Polym. Eng. Sci.* 1988, **28**, 1405
64 Mustedt, H. *Polym. Eng. Sci.* 1981, **21**, 259
65 Khan, S. and Prud'homme, R. K. *Rev. Chem. Eng.* 1987, **4**, 205
66 Work, J. L. *Polym. Eng. Sci.* 1973, **13**, 52
67 Avgeropoulos, G. N., Weissert, F. C., Biddison, P. H. and Bohm, G. G. A. *Rubber Chem. Tech.* 1975, **49**, 93
68 Paul, D. R. and Barlow, J. W. *J. Macromol. Sci.–Rev. Macromol. Chem.* (*C*) 1980, **18**, 109
69 Jordhamo, G. M., Manson, J. A. and Sperling, L. H. *Polym. Eng. Sci.* 1986, **26**, 517
70 van Oene, H. *J. Colloid Interface Sci.* 1972, **40**, 448
71 van Oene, H. in 'Polymer Blends' (Eds D. R. Paul and S. Newman), Academic Press, New York, 1978, p. 295
72 Majumdar, B., Keskkula, H. and Paul, D. R. *Polymer* 1994, **35**, 1386, 1399